Journal of Marine Research, 49, 517–542, 1991

The influence of a changing bacterial community on trace metal scavenging in a deep-sea particle plume

by James P. Cowen[1] and Yuan Hui Li[1]

ABSTRACT

An extensive set of particle samples was collected from the extended (nonbuoyant) hydrothermal plume, the distal remnant plume, and the adjacent waters in a transect across the Southern Juan de Fuca Ridge. Bacterial capsules comprised the primary species of particulate Mn. However, the data also showed significant shifts in the relative abundance of distinctive subpopulations of this bacterial community, as expressed by several consistently recurring capsule morphologies. The data are discussed with respect to distance from plume origins (relative plume age), total bacterial numbers, experimentally determined scavenging rate constants and total particulate and dissolved Mn. The relative distribution of one morph (Fibrous) corresponded ($r = .825$, $p < 0.001$) to that of the scavenging rate constant, k_1 (Cowen *et al.,* 1990) for dissolved Mn onto particles. The greatest Mn deposits (by a factor of over 10×) were associated with this same morph, which was also the numerically dominant capsule morph at the off-axis stations where total particulate Mn plume values were highest.

The disequilibrium in the particle population and the geochemical cycle of Mn in an evolving hydrothermal vent plume is reflected in the distribution coefficients for Mn (K_D), which increase with distance from vent origins. The potential influence that changing subpopulations of bacteria may exert on the overall scavenging behavior of Mn in this evolving natural particle population is emphasized.

1. Introduction

The image of the ocean as a self-regulating biogeochemical system is increasingly pervasive in discussions of the composition of ocean water. Microorganisms participate vigorously in this modulation of the ocean's composition through their crucial roles in the transformation, recycling, transport and removal of elements in ocean waters. Manganese provides an important and exceedingly interesting example of a trace constituent of seawater whose aquatic fate appears to be dominated by microbial mediation. Mn is both an essential micronutrient and a valuable tracer of geochemical processes (Bolger *et al.,* 1978; Klinkhammer, 1980; Baker *et al.,* 1985; Landing and Bruland, 1987). Furthermore, manganese chemistry also appears to

1. Department of Oceanography, School of Ocean and Earth Science and Technology, University of Hawaii-Manoa, Honolulu, Hawaii 96822, U.S.A.

exert significant control over a suite of other trace elements including Cu, Co, Ni, Zn, Pb, Cd, and Ba (Balistrieri and Murray, 1986).

In natural waters Mn is partitioned between dissolved and particulate phases, largely controlled by redox transitions between soluble Mn(II) ions and insoluble Mn(III) and Mn(IV) oxides (Hastings and Emerson, 1986). Mn(II) is thermodynamically unstable with respect to oxidation by O_2, but abiotic chemical rates of oxidation are extremely slow under normal seawater conditions (pH < 9) (Sung and Morgan, 1981). However, these rates are greatly accelerated via microbial mediation and such mediation appears to dominate the scavenging and oxidation of dissolved manganese (II) onto particles throughout the open ocean water column (Emerson *et al.,* 1982; Tebo *et al.,* 1984; Tebo and Emerson, 1985; Cowen and Bruland, 1985; Cowen *et al.,* 1986, 1990; Cowen, 1989; Mandernack and Tebo, 1988; Sunda and Huntsman, 1988). Supporting evidence includes radiotracer scavenging studies (Tebo *et al.,* 1984; Tebo and Emerson, 1985; Sunda and Huntsman, 1988; Cowen *et al.,* 1990), as well as reports that bacteria with external capsules (stable glycocalxes, Costerton *et al.,* 1981) and associated metal deposits, characteristic of many Mn oxidizing bacteria, appear to be ubiquitous in the mid- and deep-depths of the Pacific ocean (Nealson, 1983; Cowen and Silver, 1984; Cowen and Bruland, 1985).

Recently, Cowen *et al.* (1990) reported that the first order scavenging rate constant, k_1, of dissolved Mn (DMn) onto particles in a hydrothermal vent plume was inversely correlated with DMn, particulate Fe (PFe) and total suspended matter (TSM). The total k_1, as well as the fractional contribution from direct (metabolic) microbial activity were also inversely correlated with bacterial biomass in the plume. These and other data suggested that Mn scavenging within the extended plume may be dominated by a subpopulation of specialized bacteria rather than the general population of particles (TSM).

The rate of trace metal sorption by particles is a complex function of the dissolved metal concentration and the concentration and nature of the particles (Neihof and Loeb, 1974; Loeb and Neihof, 1977; Balistrieri *et al.,* 1981; Li *et al.,* 1984; Balistrieri and Murray, 1986; Honeyman *et al.,* 1988a,b; Jannasch *et al.,* 1988). Honeyman and Santchi (1988) noted that overall sorption rate constants are "smaller than expected from physicochemical theory or laboratory kinetic experiments." This behavior may be explained by surface site heterogeneity, particle interaction effects and biological activity. However, surface site heterogeneity, or sorption site concentration, is difficult to establish in field studies and particle mass concentration is usually used as a convenient, albeit inadequate, substitute (Honeyman *et al.,* 1988a,b). Particle-particle interactions are usually lost in the operationally defined terms of filterable "particulate" and filtered "dissolved" fractions (Di Torro *et al.,* 1986; Higgo and Rees, 1986; Morel and Gschwend, 1987; Honeyman and Sanchi, 1989); whereas, biological involvement is often inferred from positive correlation with biogenic

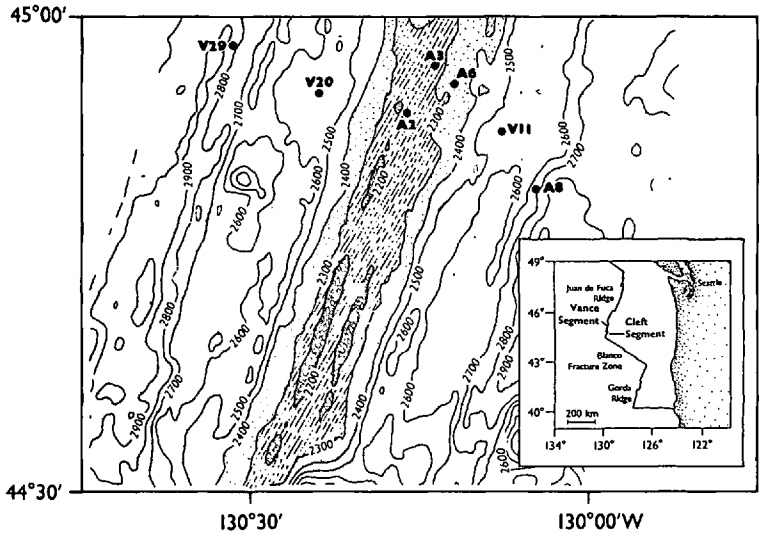

Figure 1. Map showing locations of sampling stations in vicinity of the Cleft Segment (CS), Juan de Fuca Ridge. Filled square indicates center of "Megaplume 1" (Baker *et al.*, 1987). Inset shows the study area in relation to Northern Pacific spreading center and northwestern U.S. coastline.

materials (Bishop and Fleisher, 1987) or biologic processes such as productivity (Coale and Bruland, 1985).

In this paper, we emphasize the potential influence that a changing subpopulation of metal depositing capsuled bacteria may exert on the overall scavenging behavior of Mn in a natural, heterogeneous particle population. We present the results of individual particle examination and micro-analysis of the particle population from an extended hydrothermal plume and adjacent waters. The data are discussed in terms of the major impact that specific bacterial subpopulations may have on trace element scavenging in an evolving geochemical system. This study was part of the multidisciplinary "VENTS" Program of the Pacific Marine Environmental Laboratory, NOAA, at the Southern Juan de Fuca Ridge, during the years 1987–1988.

2. Methods

a. Study area. The data discussed here are derived from studies conducted in the vicinity of the Cleft Segment (CS) of the Juan de Fuca Ridge, which is located approximately 300 km west of the Oregon coast (Fig. 1). The CS ridgecrest has been described by Normark *et al.* (1983), Koppel and Ryan (1986) and Koppel and Normark (1987). Detailed observations of the south CS vent fields centered at 44°40'N, have been reported by the USGS Juan de Fuca Group (1986) and Normark *et al.* (1987) and of the north CS vent fields by Embley *et al.* (1988). The sampling and experimental stations were located both within and outside of the CS vent fields at

the southern end of the Juan de Fuca Ridge. In this region the ridge wall rises 150 m above the axial valley floor which has a depth of about 2270 m. Plumes studied in this area since 1985 have been described by Cowen *et al.* (1986; 1990), Baker and Massoth (1986), Baker *et al.* (1987), Massoth *et al.* (1988) and Baker *et al.* (1989). Data described in this paper come primarily from seven vertical profiles collected along a cross-axis transect including 3 on-axis stations (A-2, A-3, and A-6) and 4 off-axis stations (V-29, V-20, V-11 and A-8) (Fig. 1).

b. Sampling. Selective sampling of the hydrothermal plume and adjacent waters was aided by a sensitive electronics package including sensors for conductivity, temperature, depth, light attenuation and altitude (Baker *et al.,* 1985). The plumes were identified in real time by the presence of temperature and light attenuation anomalies (Lupton *et al.,* 1985; Baker *et al.,* 1985). The rosette mounted 30-1 Niskin (General Oceanics) bottles were internally coated with teflon and fitted with teflon stopcocks and silastic closures.

Water samples intended for individual particle microanalysis were filtered through 0.2 μm Nuclepore membrane filters. Seven to 20 liters were used depending on the particle loading. Filters were then carefully "scraped" using a soft rubber spatula under a fine stream of 2% gluteraldehyde-seawater solution. Even the finest particles were thus quantitatively rinsed from the filter into 1.5 ml centrifuge tubes, as evidenced by examination of representative filters with a scanning electron microscope. Further sample preparation followed the procedures described by Cowen and Bruland (1985) as modified from Silver and Bruland (1981). Basically, the particles were further concentrated into a soft pellet by ultracentrifugation and immobilized in agar, followed by infiltration and embedding in plastic resin (Ringo *et al.,* 1979) and thin sectioned with an ultra-microtome to silver-yellow sections (~ 85 nm thick). The sections were placed onto formvar coated copper grids.

Replicate portions of each agar block were treated somewhat differently depending on the type of analysis to be done. Samples for enumeration of capsule and uncapsuled bacterial numbers were stained with ruthenium red (Luft, 1966), secondarily fixed with 1% osmium tetroxide solution and post-sectioned stained with uranyl acetate and lead citrate as described in Cowen and Bruland (1985). Samples for microanalysis, however, were directly embedded into resin without osmium, ruthenium red or post-sectioning stains. All grids were finally coated with an ultra-thin coat of high purity carbon for stability under the electron beam. Grids were examined under a Hitachi H-600 Scanning Transmission Electron Microscope (STEM) equiped with a PGT 4-Plus energy dispersive X-ray fluorescence spectrometer (EDS). An accelerating voltage of 50 kV was used as a best compromise between optimal count rate and spatial resolution.

The ratio of capsuled bacteria to total bacteria was determined using the methods of Silver and Bruland (1981) to convert TEM counts to probable numbers. The

average standard deviation for counts of multiple subsamples (ave. $n = 4$) was 17.6% (range, 2–46%). Independent direct counts of total bacteria were made using epifluorescent microscopy and the fluorescent stain 4'6-diamidino-2-phenylindole (DAPI) (Porter and Feig, 1980). Standard deviations for the epiflourescent direct counts of total bacteria averaged 14% (range, 9–24%); about 1000 cells were counted for each sample. The product of the value from the direct counts of total bacteria and the ratio of capsuled bacteria to total bacteria provided an estimate of the actual number of capsuled bacteria per ml of seawater.

Micro-analyses were performed on portions of unstained sectioned particles occupying the reduced rastor at 50 K times magnification. Semi-quantitative Mn:Fe ratios were derived from the background (continuum) subtracted peak integrals. The concentration of Mn in the analysis volume (i.e., the portion of the thin sectioned sample analyzed), C_{av}, was determined by a with-standards form (Princeton Gamma-Tech, Inc.) of the Hall continuum method (Hall, 1971; 1979a,b; Hall and Gupta, 1979). Standards were made by dissolving an organo-metalic complex (tricarbonyl-methylcyclopentadienyl-Mn) in the same embedding resin used in sample preparation. There was no detectible Mn in the embedding resin (EDS detection limits were 0.1 mass percent). Therefore, the concentration of Mn actually associated with the bacterial capsule, was better approximated by dividing the Mn concentration in the analysis volume by the fraction of the analysis volume contributed by capsular material, a_f,

$$\mu g\ Mn/\mu g\ capsule = C_{av} a_f^{-1}. \quad (1)$$

The fraction, a_f, was routinely determined using standard digital imaging techniques and commercially available software (PG-T, Inc.). Estimates of entire capsule volumes, V_{cap}, were extrapolated from cross-sectional areas of the thin-sectioned capsules as determined by digital imaging feature analysis.

The quantitative micro-analysis data are presented in three ways: Mn:Fe ratios; normalized to unit capsule polymer mass (Eq. 1); and normalized to the whole individual capsule (Mn per capsule).

3. Results and discussion

a. Dominant species of particulate Mn. Our data indicate that the extracellular capsules produced by many metal-depositing bacteria comprise the primary species of particulate Mn in the waters studied. Furthermore, the association of metal deposits and exo-polymers result in several consistently recurring morphological classes of capsules (Fig. 2). Mn was strongly associated with bacterial capsules, but was undetectable in noncapsule particles collected from the extended plume using EDS microanalysis techniques. The digital elemental dot maps in Figure 3 show the distribution of several elements with respect to one such capsule and a group of amorphous FeOOH particles. Note that whereas the Fe is clearly associated with

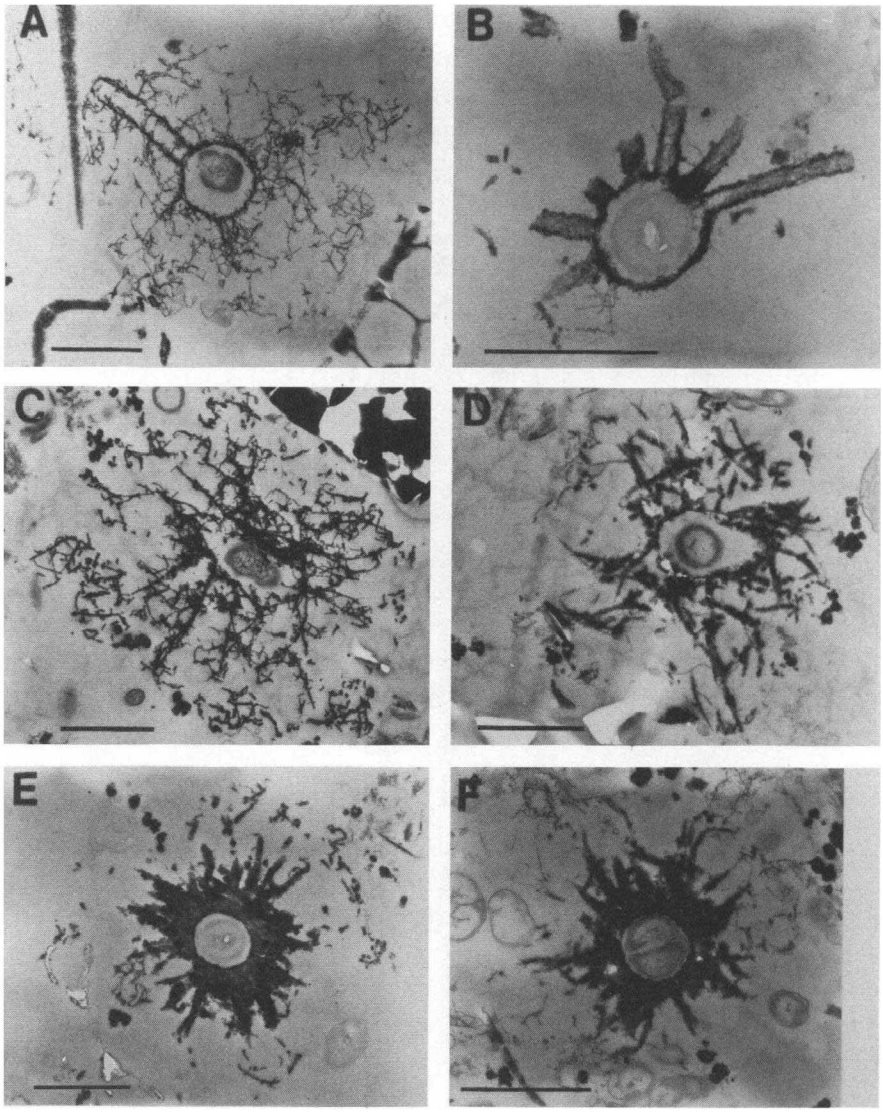

Figure 2. TEM micrographs of the three dominant extracellular capsule morphs. (a and b) "Budding" capsules; (c and d) "Fibrous" capsules; and (e and f) "Star" capsules.

both the capsule and FeOOH particles, Mn is detectible on the capsule only. Also shown is phosphorus which is believed to be co-scavenged with the iron (Feely *et al.*, 1990).

The detection limits for Mn in this technique is about 0.1 wt % (1000 $\mu g\ g^{-1}$). On the other hand, the potential contribution from other abundant particles that possess Mn concentrations below this EDS detection level does not appear to be major. If the conservative assumptions are made that all PFe was in the form of FeOOH and

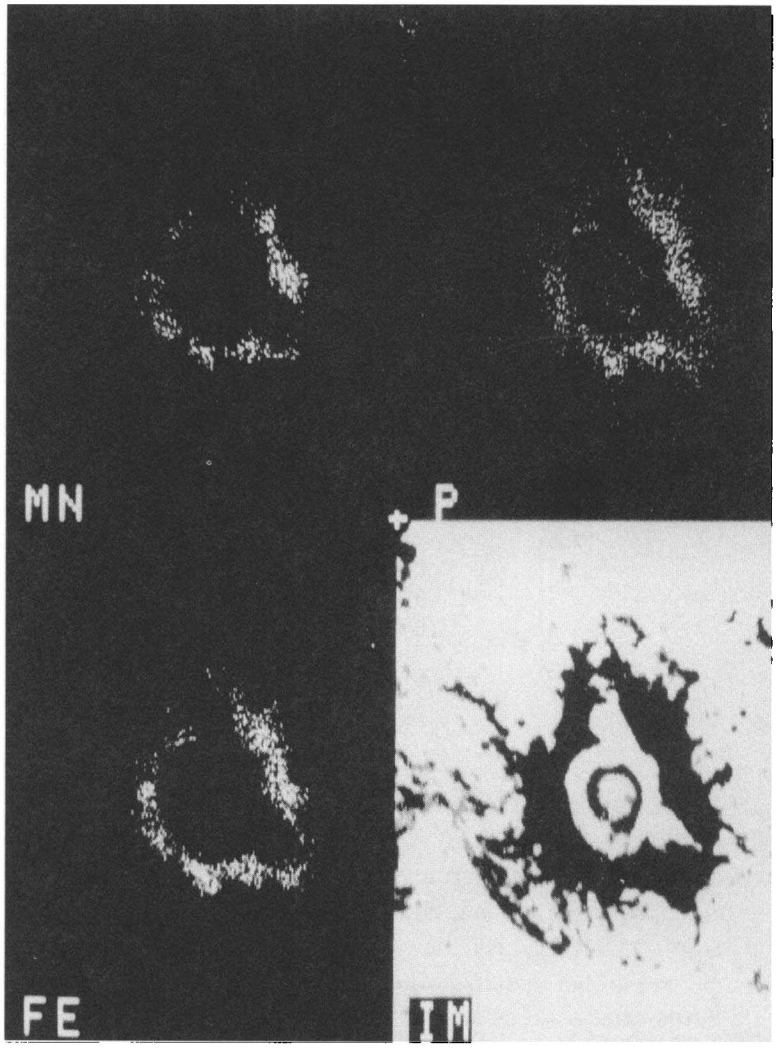

Figure 3. Digital elemental dot maps of a bacterial capsule (center) and amorphous FeOOH particles. (a) Mn map; (b) P map; (c) Fe map; and (d) a digitized TEM image.

that the Mn content of the particulate FeOOH's was as much as 1000 $\mu g\ g^{-1}$, then the maximum contribution from PFe to total PMn would have been less than 15%, considerably less at off-axis stations (Table 1). Extending similar assumptions to total suspended matter concentrations (Cowen *et al.,* 1990) would still account for generally less than 50% of the measured PMn at on-axis stations and less than 25% at off-axis stations (Table 2). The implication of this exercise is made even clearer if it is considered that the concentration of PMn is negatively correlated to those of PFe and TSM. Therefore, the majority of the PMn must be selectively concentrated into particles at levels significantly higher than EDS detection levels.

Table 1. Maximum contribution of particulate FeOOH to total particulate Mn.

	Measured Tot. PFe		Particulate Mn Max Contrib. from p-FeOOH		Meas. Tot. p-Mn	%Mn Contrib. from
Depth	nM-Fe L^{-1}†	Equivalent μg FeOOH L^{-1}	ng L^{-1}	nM L^{-1}	nM L^{-1}†	p-FeOOH
On Axis Sta A-2						
1925	10	0.9	0.9	0.02	1.5	1%
2025	41	3.6	3.6	0.06	1.5	4
2075	94	8.4	8.4	0.15	1.2	12
2125	97	8.6	8.6	0.16	1.1	14
2175	88	7.8	7.8	0.14	1.4	10
2250	67	6.0	6.0	0.11	1.9	6
Off-Axis Sta A-8						
1925	4	0.36	0.36	0.007	1.2	0.6
1975	4	0.36	0.36	0.007	1.5	0.5
2075	7	0.62	0.62	0.011	2.1	0.5
2125	6	0.53	0.53	0.010	2.5	0.4
2175	6	0.53	0.53	0.010	2.5	0.4
2225	7	0.62	0.62	0.011	3.4	0.3

†Data from Cowen *et al.*, 1990.

b. On- versus off-axis shifts in bacterial subpopulations. The total numbers of bacteria were greatly elevated at the stations nearest to known active vent fields (on-axis), but at most off-axis stations, 10–20 km distance from the vent fields, they had returned to levels indistinguishable from background (Table 3) (Fig. 4a). The on-axis stations showed a pronounced maximum in total bacteria in the depth range of 1900–2250 m, with numbers up to 15×10^4 cells ml^{-1}. This depth range was consistent with the maxima in total suspended matter, particulate Fe and dissolved Mn (Cowen *et al.*, 1990) found at the same stations and defined the vertical extent of the nonbuoyant hydrothermal plume eminating from the on-axis vent fields. The combined off-axis data (except V-II, see below) showed a rather flat profile throughout the sample depth range; bacterial numbers varied little from about 5×10^4 cells ml^{-1}. Elevated total bacterial biomass in hydrothermal plumes have been reported previously primarily for hydrothermal effluents (Karl *et al.*, 1980; Tuttle *et al.*, 1983; Winn *et al.*, 1986) but also for the proximal regions of the nonbuoyant portion of plume SJFR (Winn *et al.*, 1986; Cowen *et al.*, 1986). The attrition in total numbers with distance from the vent fields can be explained by a combination of dilution of the spreading plume and loss due to predation and vertical transport.

Sta. V-11 is clearly an exception to the trends observed in the other off-axis stations. The plume depths at V-11 were characterized by moderately high DMn and PFe, low PMn and high numbers of bacteria. This anomalous station reflects the

Table 2. Maximum contribution of total suspended matter (TSM) to total particulate Mn.

		Particulate Mn			
Depth	Measured TSM ($\mu g\ L^{-1}$)†	Max. Contrib. from TSM ($ng\ L^{-1}$)	($nM\ L^{-1}$)	Measured Tot. PMn ($nM\ L^{-1}$)†	%Mn Contrib. from Tot. TSM
On-Axis Sta. A-2					
1925	20	20	0.36	1.5	24%
2025	19	19	0.34	1.5	23
2075	31	31	0.56	1.2	47
2125	33	33	0.60	1.1	54
2175	27	27	0.49	1.4	35
2250	23	23	0.41	1.9	22
Off-Axis Sta A-8					
1925	10.5	10.5	0.19	1.2	16
1975	20.5	20.5	0.37	1.5	25
2075	13	13	0.24	2.1	11
2125	13	13	0.24	2.5	10
2175	13	13	0.24	2.5	10
2225	13	13	0.24	3.4	7

†Data from Cowen *et al.*, 1990.

vagrancies of the mid-depth currents in the vicinity of the SJFR (Cannon and Pashinski, 1990; Baker *et al.*, 1989) and, by extension, the difficulty in relating the relative age of spreading hydrothermal plumes to distance from active venting areas (Cowen *et al.*, 1990). A more consistent indicator of plume age appears to be the partitioning of manganese between dissolved and particulate phases (Klinkhammer *et al.*, 1985; Klinkhammer and Hudson, 1986). Hydrothermal Mn is discharged to the oxygenated bottom waters as dissolved Mn^{+2}, but gradually converts to the particulate phase through scavenging and oxidation. Hence, the data on bacterial subpopulations (Table 4) have been plotted versus the proportion of manganese present as particles; a higher particulate proportion should indicate an older plume (Fig. 4b; Fig. 5–8). By this criteria, plume depth waters at Sta. A-2, A-3, A-6, and V-11 would be relatively young, and those at Sta. A-8, V-20, and V-29 old.

The data show a shift in the relative abundance of certain subpopulations of the bacterial community relative to apparent plume age. Total numbers of capsuled bacteria were elevated at plume depths at all stations (Table 3). At these depths total capsules were more numerous in young plume waters ($1–2.3 \times 10^4$ cells ml^{-1}) than in more mature plumes ($\sim 0.7 \times 10^4$ cells ml^{-1}); although, this was primarily due to the greatly enriched general bacterial population in the young plume water. By comparison, the relative abundance (f) of the total capsules, with respect to total bacteria, showed no correlation with indicators of plume age (Fig. 5b). However, specific

Table 3. Numbers of total bacteria (Bact), total capsules (T Cap), "budding" capsules (BUD), "FM" capsules (FM), and "star" capsules (STAR); capsule fractions of total bacterial population (f); particular Fe and Mn; and dissolved Mn scavenging rate constant, k_1.

Station	Depth (m)	no. (thousands) per ml					f (capsule/bacteria)				PMn* (nM/L)	PFe* (nM/L)	k_1^* (1/yr)
		BACT	BUD	FM	STAR	T CAP	BUD	FM	STAR	T CAP			
A-2	999	72	0.0	2.4	0.00	2.4	0.000	0.033	0.000	0.033	0.2	2	—
	1348	83	0.4	1.9	0.27	2.5	0.005	0.023	0.003	0.030	0.2	3	—
	1549	71	8.1	6.7	0.31	14.5	0.115	0.095	0.004	0.205	0.3	3	—
	1902	91	7.2	6.1	0.70	13.6	0.079	0.067	0.008	0.149	1.6	9	0.43
	1950	132	13.8	11.2	0.52	24.9	0.104	0.085	0.004	0.188	1.7	16	0.16
	2003	208	9.4	5.2	0.00	14.4	0.045	0.025	0.000	0.069	1.7	32	0.04
	2051	161	12.9	12.0	0.23	24.6	0.080	0.075	0.001	0.152	1.5	67	0.07
	2103	154	13.9	5.7	0.65	19.5	0.090	0.037	0.004	0.127	1.3	96	0.09
A-3	1250	87	0.8	2.5	0.00	3.3	0.009	0.029	0.000	0.038	—	—	—
	1500	71	1.0	4.4	0.36	5.7	0.014	0.062	0.005	0.080	0.5	3	—
	1749	71	3.5	7.1	0.35	10.8	0.049	0.100	0.005	0.151	0.8	4	—
	1905	64	4.4	5.1	0.16	9.4	0.068	0.079	0.002	0.146	1.6	7	0.80
	1948	140	5.2	4.5	0.00	9.6	0.038	0.032	0.000	0.069	1.9	13	0.06
	1995	149	6.3	2.6	0.00	8.9	0.043	0.018	0.000	0.060	1.5	35	—
	2051	140	8.3	4.2	0.21	12.5	0.059	0.030	0.001	0.090	1.6	45	0.03
	2097	109	6.6	4.6	0.11	11.2	0.060	0.042	0.001	0.102	1.3	125	0.05
	2098	136	15.1	7.3	0.71	22.7	0.111	0.054	0.005	0.167	1.3	125	0.04
	2150	142	5.7	2.9	0.00	8.5	0.041	0.020	0.000	0.060	1.3	121	—
A-6	1250	78	0.4	4.0	0.26	4.7	0.005	0.051	0.003	0.060	0.2	2	—
	1500	80	3.7	4.9	0.16	8.7	0.046	0.062	0.002	0.109	0.3	3	—
	2000	103	5.6	5.3	0.00	10.7	0.054	0.052	0.000	0.104	1.7	29	0.12
	2100	115	6.6	3.0	0.23	9.9	0.057	0.026	0.002	0.086	1.6	87	0.17
	2150	144	6.5	4.1	0.00	10.9	0.045	0.029	0.000	0.075	1.7	72	—
	2200	120	9.8	9.6	0.00	19.0	0.082	0.080	0.000	0.159	1.9	59	0.14
	2250	100	6.2	5.1	0.45	11.5	0.062	0.051	0.004	0.116	—	—	0.49

Table 3. (Continued)

Station	Depth (m)	no. (thousands) per ml BACT	BUD	FM	STAR	T CAP	*f* (capsule/bacteria) BUD	FM	STAR	T CAP	PMn* (nM/L)	PFe* (nM/L)	k_1^* (1/yr)
V-29	1250	65	0.0	1.2	0.15	1.4	0.000	0.018	0.002	0.021	—	—	—
	1900	64	2.0	7.0	0.98	9.9	0.031	0.110	0.015	0.155	1.5	7	—
	1900	53	1.4	3.8	0.32	5.5	0.027	0.072	0.006	0.103	1.5	7	—
	2050	51	2.6	6.7	0.63	9.7	0.050	0.131	0.012	0.189	1.8	8	—
	2054	48	2.9	4.9	0.51	8.0	0.061	0.101	0.011	0.168	1.8	8	1.97
	2206	51	1.7	7.7	0.46	9.7	0.034	0.153	0.009	0.192	2.3	8	3.22
V-20	1500	48	0.5	1.6	0.05	2.1	0.010	0.033	0.001	0.043	—	—	—
	1750	39	1.8	4.3	0.33	6.3	0.046	0.109	0.008	0.160	—	—	—
	2000	41	2.2	4.7	0.44	7.2	0.054	0.115	0.011	0.175	—	—	1.50
	2000	33	1.1	3.4	0.23	4.6	0.032	0.105	0.007	0.142	—	—	1.50
	2050	29	1.9	3.0	0.36	5.1	0.066	0.104	0.013	0.178	1.7	6	2.10
	2100	45	1.9	3.3	0.12	5.4	0.043	0.074	0.003	0.118	1.9	7	1.05
	2200	37	1.2	2.9	0.00	4.0	0.032	0.080	0.000	0.110	—	—	1.05
	2350	46	1.7	4.0	0.25	5.9	0.037	0.088	0.005	0.129	—	—	—
A-8	2200	61	1.3	2.8	0.06	4.3	0.021	0.047	0.001	0.071	2.7	7	1.43
	2250	70	1.1	2.7	0.35	4.3	0.016	0.039	0.005	0.062	3.3	8	—
V-11	1500	76	1.3	2.8	0.11	4.2	0.017	0.037	0.001	0.055	—	—	—
	1500	86	0.7	3.2	0.73	4.7	0.008	0.037	0.009	0.055	—	—	—
	2000	111	13.2	4.9	0.52	18.2	0.118	0.044	0.005	0.164	1.9	22	0.51
	2100	152	13.5	4.9	0.08	18.4	0.089	0.032	0.000	0.121	2.0	36	0.18
	2100	136	12.5	4.0	0.34	16.8	0.092	0.030	0.002	0.124	2.0	36	0.19
	2150	122	9.6	4.8	0.36	14.5	0.079	0.039	0.003	0.119	2.1	31	0.20

*Data from Cowen *et al.* 1990.

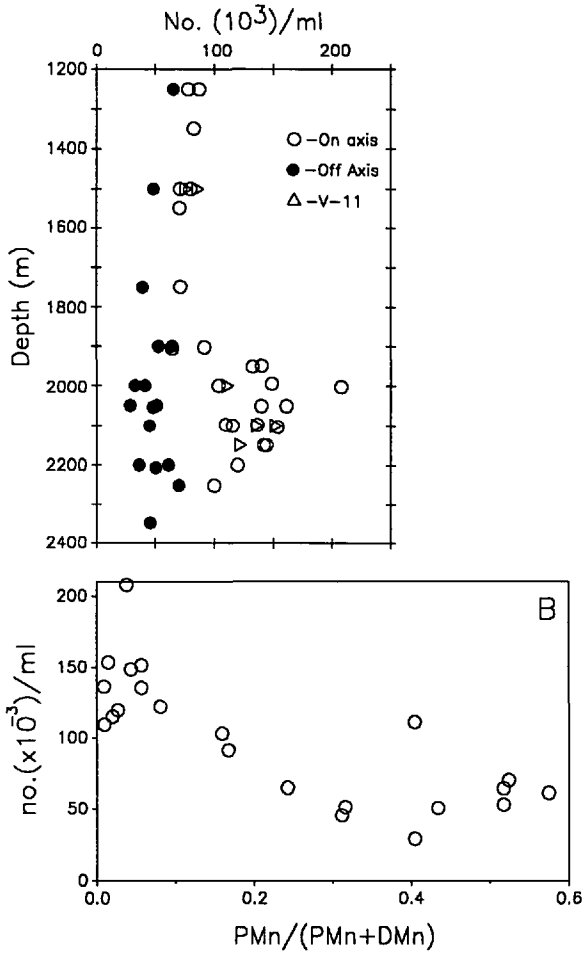

Figure 4. (a) Total number of bacteria (in thousands per ml) versus depth. In order to reveal the major trends, the data are plotted in terms of their general proximity to the presumed origins of the hydrothermal plume; that is, the data are combined into on-axis (open circles; Sta. A-2, A-3 and A-6) and off-axis groups (filled circles; Sta. V-29, V-20 and A-8). Sta. V-11 data are distinguished as triangles (see text). (b) Same bacteria number data plotted against the proportion of Mn present as particles ($r = -0.779, p < 0.001$).

major morphological classes of the capsules exhibited more pronounced, and contrasting, trends in their numerical abundance. The distribution of the "Budding" capsule morph (Fig. 6a) reflected that of the total bacteria; they were clearly more abundant in young plume waters than in mature plumes, both numerically (Fig. 6a) and relative to total bacteria (Fig. 6b). In fact, this capsule morph appeared to be relatively more abundant, with respect to total bacteria numbers, at plume depths than at nonplume depths for all stations. In young plumes, the "Budding" capsule morph also tended to be the most abundant morph at plume depths.

Table 4. Distribution coefficients, K_D, of Mn between dissolved and particulate phases and the first order scavenging and desorption constants k_1 and k_2.

Station	Depth (m)	PMn* (nM/l)	DMn* (nM/l)	TSM* (μg/l)	Log K_D (l/kg)	k_1 (yr^{-1})	k_2 (yr^{-1})	k_1/k_2
V-29	1520	0.2	1.0	13.5	7.2			
20 km W	1900	1.2	1.4	12.5	7.8			
	2000	1.6	3.8	12	7.5			
	2100	1.6	4.0	13	7.5	2.4	5.8	0.41
	2250	2.4	2.4	15	7.8	3.3	3.5	0.94
V-20	2024	1.6	2.5	9.3	7.8	1.8	3.1	0.58
10 km W	2100	2.0	4.2	9.6	7.7	1.0	2.1	0.48
	2250	2.9	3.5	17	7.7			
A-2	1500	0.3	0.8	10	7.6			
<1 km	1900	1.8	8	18	8.1	0.43		
	2000	1.8	43	18	7.4	0.04		
	2100	1.2	86	32	6.6			
	2200	1.9	50	22	7.2	0.09		
A-3	1569	0.5	1.6	28	7.1			
<1 km	1900	1.7	5.0	9	7.6	0.8		
	2000	1.6	33.0	24	6.3	0.06		
	2100	1.3	140	33	5.4	0.04		
	2250	1.5	72	29	5.9			
A-6	1500	0.2	1.3	12	8.2			
3.5 km	1900	1.8	5	11	8.5			
	2000	1.8	9	12	7.2	0.12		
	2100	1.5	78	27	5.8	0.17		
	2200	1.9	70	23	6.1	0.14		
	2250	2.9	24	33	6.6	0.49		
V-11	1900	1.4	3.0	10	7.6			
10 km E	2000	1.8	2.8	12	7.7	0.51		
	2100	2.0	33	15	6.6	0.18		
	2200	2.0	15.3	15	6.9			
	2250	2.8	12	17	7.1			
A-8	1500	0.4	0.7	10	7.7			
16 km E	1900	1.2	0.7	10	8.2			
	2000	1.3	2.1	21	7.4			
	2100	2.4	5.0	12	7.6			
	2200	3.2	2.0	12	8.1	1.4	0.93	1.5
	2250	3.4	3.0	12	8.0			

*Data from Cowen *et al.*, 1990.

On the other hand, the trends in the plume age-related distribution of the "Fibrous" and "Star" capsules were counter to that of the total bacterial biomass. The numerical abundance of the "Fibrous" capsule morph (Fig. 3c,d) showed no correlation to our plume age indicator (Fig. 7a). This is especially significant in light of the sharp trend observed in the overall bacterial numbers (Fig. 4b). In fact, the

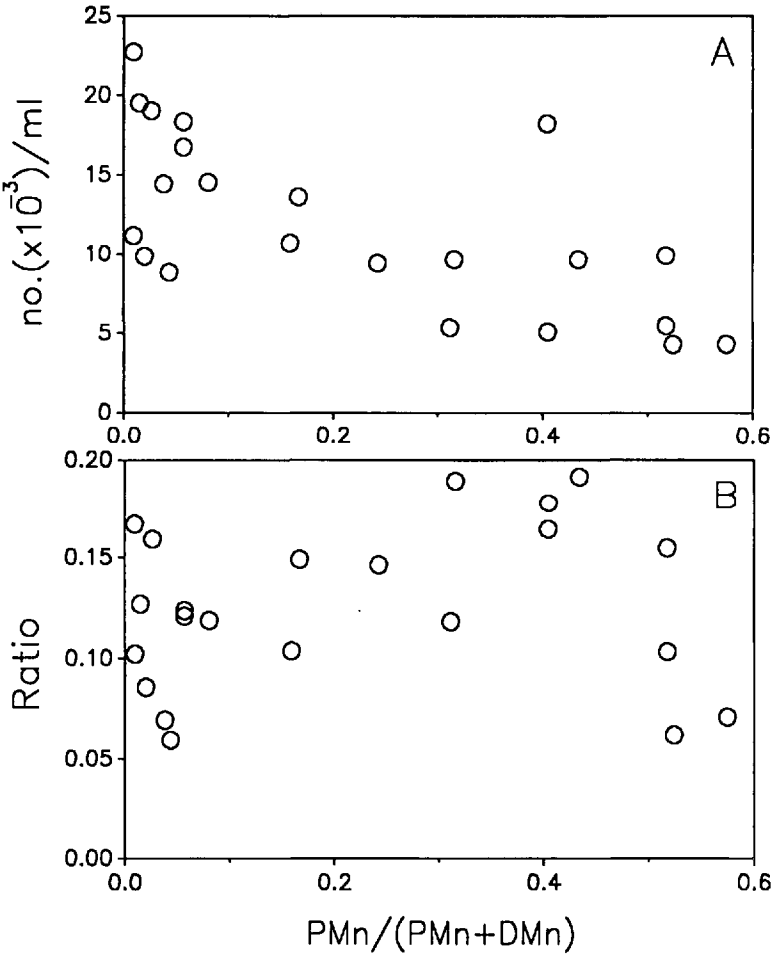

Figure 5. Numbers of total capsules (a) and the relative abundance of total capsules with respect to total bacteria (b) versus the proportion of Mn present as particles (a: $r = -0.669$, $p < 0.01$; b: $r = 0.122$, no correl.).

relative abundance of the "Fibrous" capsule morph at plume depths tended to be greater in older plume than young plume waters (Fig. 7b). Finally, the distributions for both the numerical and relative abundance of the "Star" capsule morph (Fig. 8a,b) were very similar to those of the "Fibrous" morph. Therefore, either these two capsule morphs are being produced within the plume at an accelerated rate relative to the general bacterial population, or they are surviving the various attrition factors preferentially to the other bacteria. It should be noted that although the "Star" morph appeared to show a slight maximum in numerical abundance at both on- and off-axis stations (Table 3), they were an order of magnitude less abundant than either the "Budding" or "Fibrous" capsules.

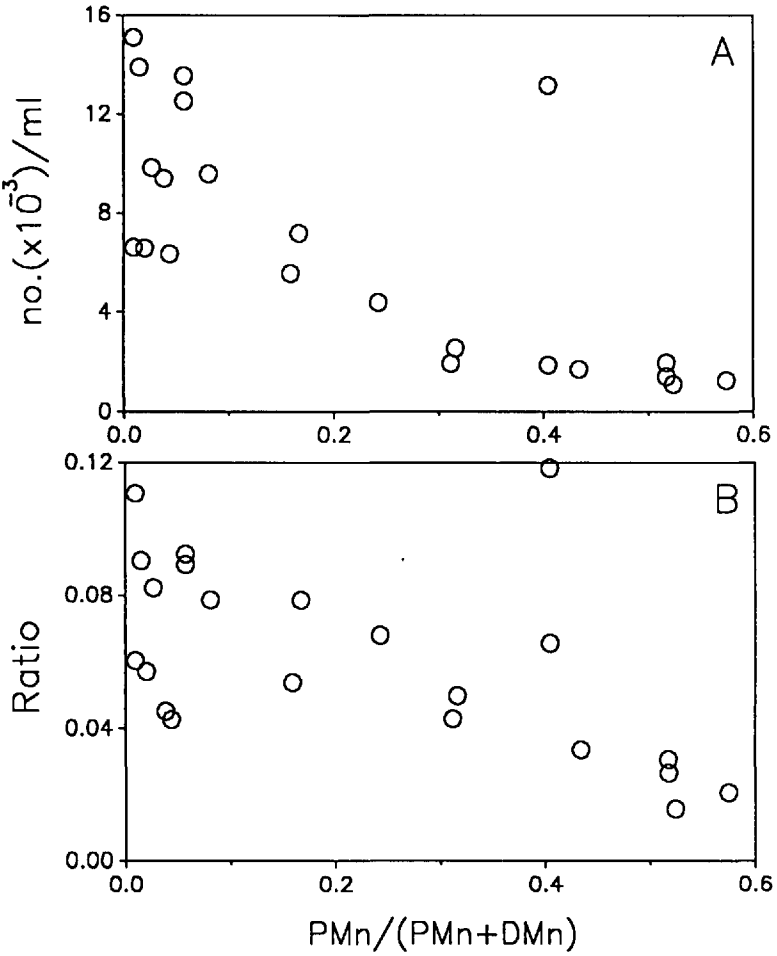

Figure 6. Numbers of "Budding" capsules (a) and the relative abundance of "Budding" capsules with respect to total bacteria (b) versus the proportion of Mn present as particles (a: $r = -0.729, p < 0.001$; b: $r = -0.575, p < 0.01$).

c. Implications for scavenging models. The potential importance of this compositional shift in the microbial population is emphasized by the difference in Mn loading between the two most abundant capsule morphs. The average "Fibrous" capsule analyzed possessed over an order of magnitude greater Mn deposits than did the average "Budding" capsule (Fig. 9a). The "Fibrous" capsules' more intense Mn deposits per unit of capsule mass (Fig. 9b) and their greater capsule size accounted for the substantial difference in Mn loading. The difference between capsule morphs in the amount of Mn deposits per unit of capsule is more difficult to explain. The "Fibrous" capsules had on the average 2–5 times more Mn per unit capsule mass than did the "Budding" capsule morphs. The consistently higher Mn:Fe ratio found

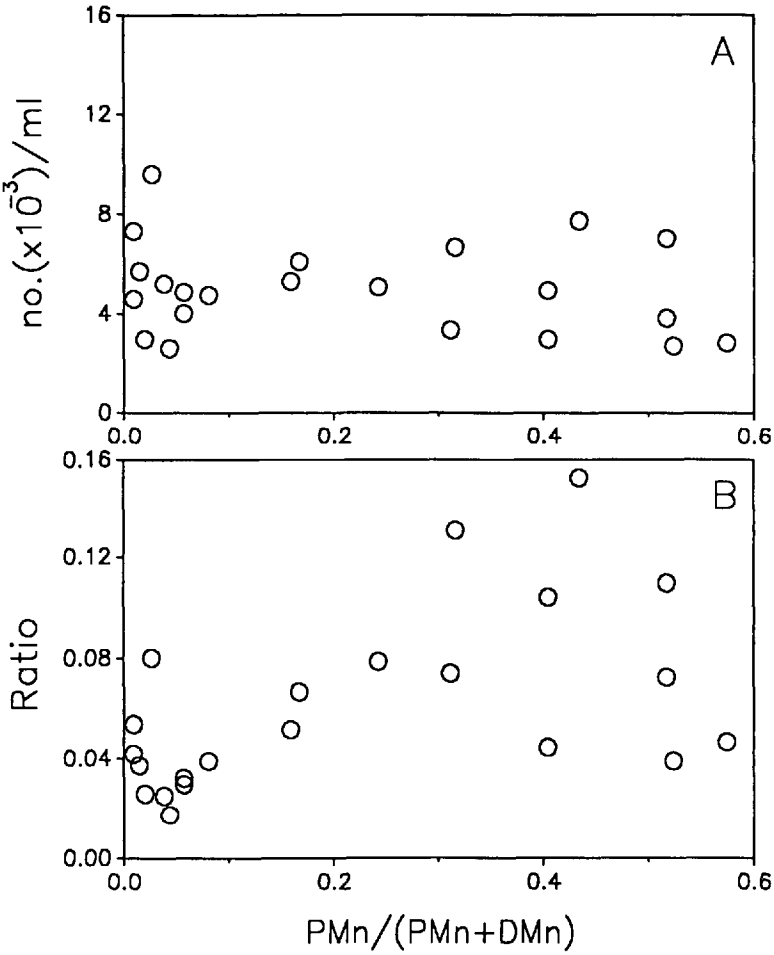

Figure 7. Numbers of "Fibrous" capsules (a) and the relative abundance of "Fibrous" capsules with respect to total bacteria (b) versus the proportion of Mn present as particles (a: $r = 0.190$, no correl.; b: $r = 0.516, p < 0.02$).

on the "Fibrous" capsules than on the "Budding" capsules (Fig. 9c) suggests either a higher relative selectivity for Mn by the former or different scavenging mechanisms. Analogous values for the "Star" capsules (not shown) were very similar to those of the "Fibrous" capsules.

These shifts in the subpopulations of capsuled bacteria have important implications for trace metal scavenging. Trace element scavenging models are built upon measured or assumed characteristics of the relevant particle population. Frequently, bulk analyses are employed to form generalizations concerning the scavenging affinity and constancy of the particles. In the hydrothermal plume system discussed

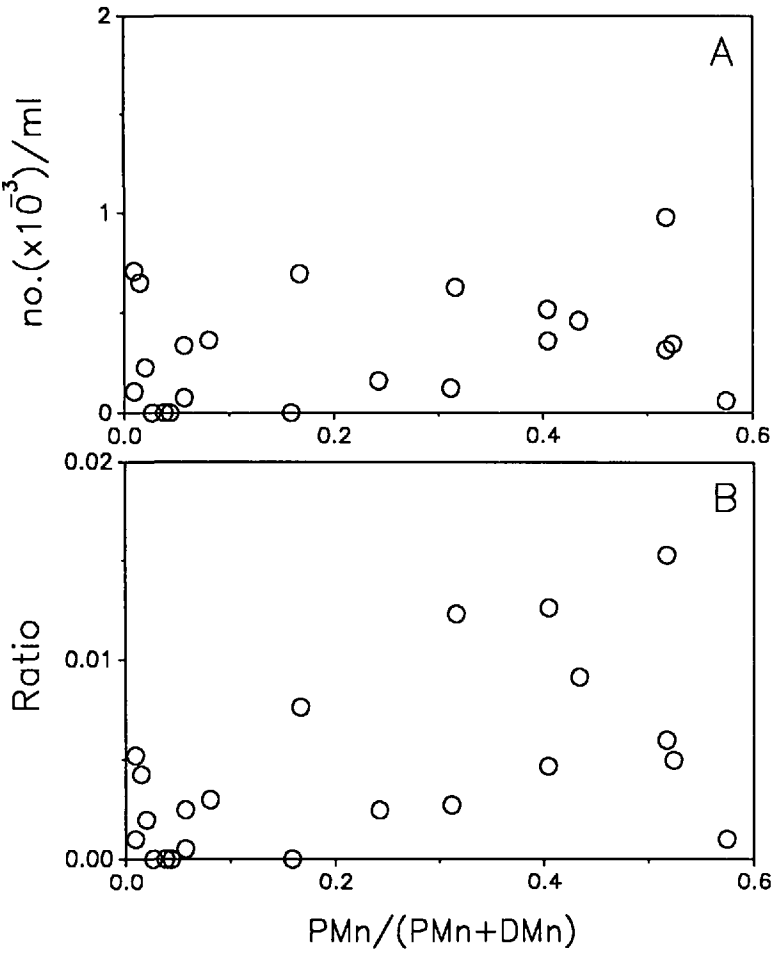

Figure 8. Numbers of "Star" capsules (a) and the relative abundance of "Star" capsules with respect to total bacteria versus the proportion of Mn present as particles (a: $r = 0.261$, no correl.; b: $r = 0.549, p < 0.02$).

here, neither the particle population nor the Mn geochemical cycle were at equilibrium. The particle populations of hydrothermal plumes were clearly dynamic, changing dramatically in both concentration and character. Particulate Fe concentrations which were dominated by amorphous FeOOH colloids clearly decreased with distance from known active vent fields (Cowen *et al.*, 1986). In addition, corresponding and contrasting trends existed in the distribution of different bacterial subpopulations described in this paper.

The disequilibrium is clearly reflected in the *in situ* distribution of Mn between its particulate and dissolved states. The distribution coefficients, K_D, increased at plume

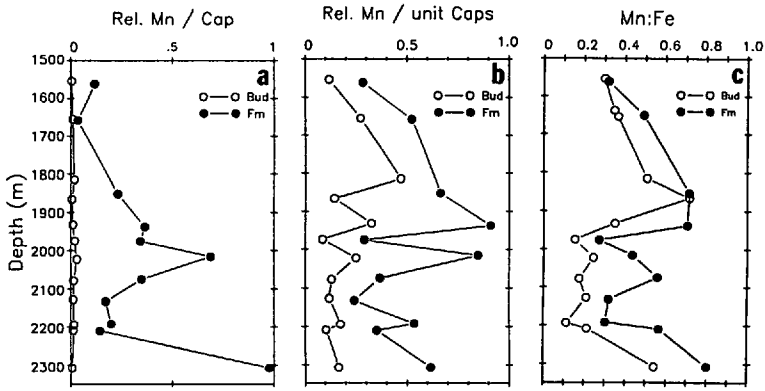

Figure 9. A comparison of the EDS elemental microanalysis results for the "Budding" and "Fibrous" capsule morphs as a function of depth from the 1987 field season at the CS, SJFR. These data were not readily separated into on- and off-axis stations. However, the comparison between the two major capsule morphs shows several important trends. Each point represents the mean value from the microanalysis of 20–50 capsules (1 sd, 50–70%). (a) the relative Mn deposit per individual capsule; (b) mean relative Mn deposit intensities per unit of capsule mass (metal deposits plus polymer); and (c) The mean Mn:Fe ratios.

depths (~ 1900–2200 m) by almost three orders of magnitude from young to older stations (Table 4) where, by definition,

$$K_D = [\text{PMn}]/([\text{DMn}][\text{TSM}]), \tag{5}$$

and [] indicates concentration. If [DMn] and [PMn] are related by the first order reaction [DMn] $\rightleftharpoons$ [PMn], the change rate of [DMn] would be:

$$d[\text{DMn}]/dt = -k_1[\text{DMn}] + k_2[\text{PMn}], \tag{6}$$

where k_1 and k_2 are, respectively, the first order scavenging and desorption rate constants. At a steady state (i.e., $d[\text{DMn}]/dt = 0$),

$$k_1/k_2 = [\text{PMn}]/[\text{DMn}] = K_D[\text{TSM}]. \tag{7}$$

Otherwise, the solution for Eq. (6) (Nyffeler *et al.,* 1984) is:

$$K_D = (1 - a)/([\text{TSM}]a), \quad \text{where}$$
$$a = (k_2/(k_1 + k_2)) + (k_1/(k_1 + k_2))e^{-(k_1+k_2)t}. \tag{8}$$

The k_1 values at various stations have been determined by radiotracer techniques (Cowen *et al.,* 1990) and are reproduced in Table 4. If one assumes that the samples from the off-plume stations are already in a steady state, the k_2 and k_1/k_2 values can be estimated from Eq. 7. The results are again summarized in Table 4. Interestingly, the k_1 and k_2 values are similar in magnitude, and the k_1/k_2 ratios range from 0.4 to 1.5. If we adopt the k_1/k_2 ratio of about one and assume the same ratio can be roughly

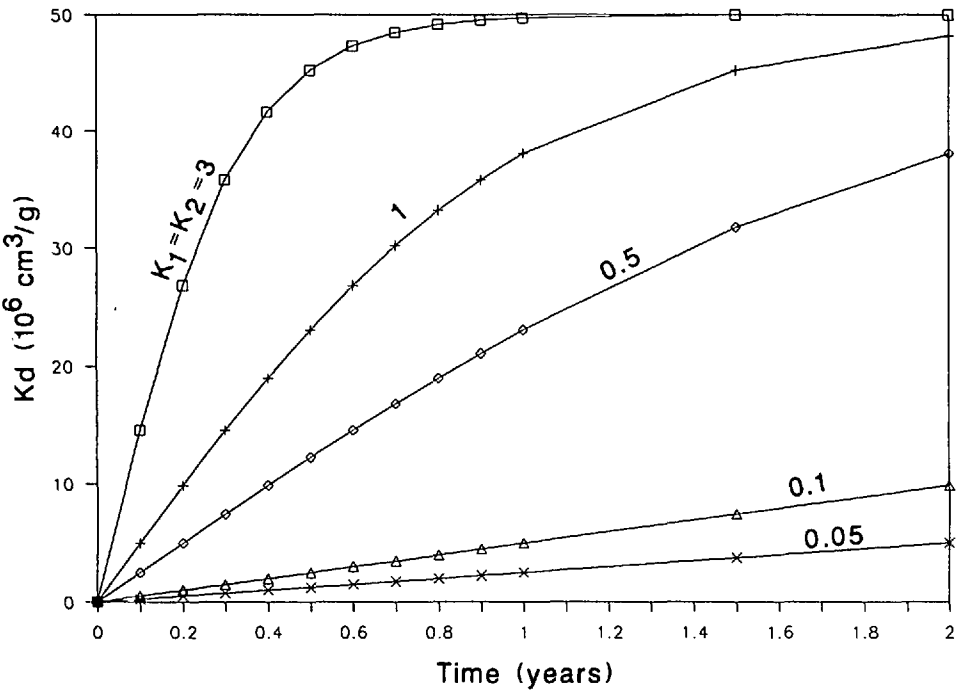

Figure 10. The K_Ds as a function of time (t) and k_1 ($=k_2$) according to Eq. 8. Total suspended matter, [TSM], is fixed at 20 $\mu g\, l^{-1}$.

applied to the on-plume stations, then, we can predict how K_D values change as functions of time (t) and k_1 (or k_2) values as exemplified in Figure 10. It is evident from Figure 10 that the K_D values of the on-plume stations (with low k_1 and k_2 values) increase only slowly and would take several years to reach an equilibrium value (ie., 5×10^7 cm^{3}g^{-1}, here).

Of course, a more realistic model for the uptake of Mn by particles is

$$[\mathrm{DMn}] \underset{k_2}{\overset{k_1}{\rightleftharpoons}} [\mathrm{PMn}] \overset{k_3}{\rightleftharpoons} [\mathrm{PPMn}],$$

where k_3 is the first order rate constant for converting reversibly adsorbed Mn into irreversibly fixed Mn (PPMn) (Nyffeler *et al.*, 1984). It is however, not feasible to estimate both k_2 and k_3 with our data base.

The important question posed by our simple model is why the k_1 (or k_2) values are higher in the off-axis plume than in the on-axis plume stations. Particles vary widely in their affinity for and capacity to scavenge metals from seawater (Davis and Leckie, 1979; Sung and Morgan, 1981; Balistrieri *et al.*, 1981; Bacon and Anderson, 1982; Li *et al.*, 1984; Balistrieri and Murray, 1984). Changes in the composition of the particle population could significantly alter the partitioning of elements between dissolved

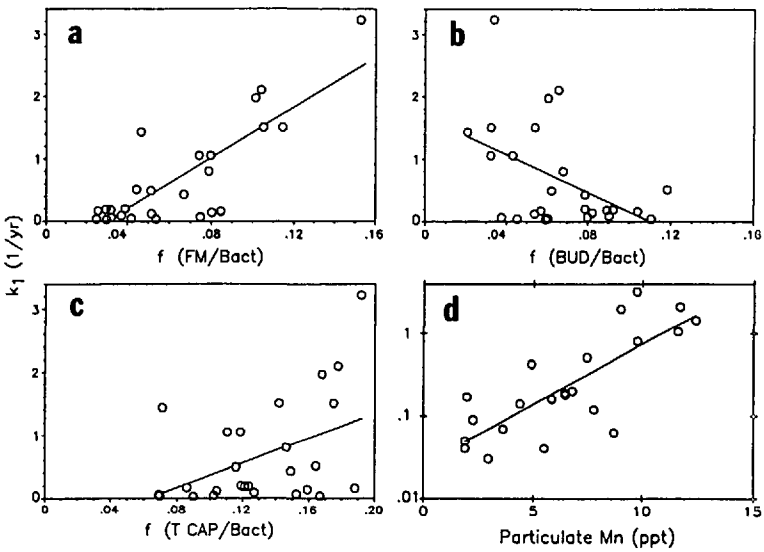

Figure 11. (a,b,c) Scatter plots of the forward scavenging rate constant, k_1, for DMn onto particles versus the subpopulation fractions, f, of the capsule morphs relative to total bacterial numbers, where f equals: (a) "fibrous" capsules/total bacteria; (b) "budding" capsules/total bacteria; (c) total capsules/total bacteria. (d) Semi-log plot of k_1 versus particulate Mn (mg/g). Correlation coefficients are given in the text. The k_1 values are from Cowen *et al.*, 1990, and listed in Table 1.

and particulate phases. Metal depositing capsuled bacteria are prominent scavengers of DMn. Their increase in proportion to the total bacterial population with increasing plume age could explain such a shift in the plume k_1 values. This hypothesis is supported by the strong positive correlation between k_1 and the "Fibrous" morph fraction of the bacterial population (Fig. 11a; $r = .825, p < 0.001$). The present data also indicate that this capsule morph accounts for the greatest proportion of suspended PMn. In contrast, k_1 is only moderately correlated to the total capsules/bacteria fraction (Fig. 11c; $r = 0.453, p < 0.05$) and is negatively correlated with the "Bud" morph fraction (Fig. 11b; $r = -0.860, p < 0.001$).

Another interesting observation is that the k_1 values are also positively correlated to the Mn concentration in suspended particles (mg/g) (Fig. 11d; $r = .787, p < .001$). A partial implication maybe that the scavenging of Mn is controlled by the autocatalytic oxidation process of manganese on MnO_2-rich particles (Stumm and Morgan, 1981; Li *et al.*, 1984), especially the "Fibrous" morph capsules. However, the initial precipitation of Mn on capsuled bacteria must be enhanced by some biochemical process. Cowen *et al.* (1990) reported that up to half of the DMn scavenged onto plume particles at Sta. A-8, V-20 and V-29 appeared to be influenced by bacterial metabolic activity.

d. Alternative bacterial scavenging mechanisms. The data described above provide clear evidence of microbially mediated trace metal scavenging. However, the more specific mechanisms by which capsuled bacteria scavenge Mn is not certain. Alternatives include (1) physicochemical processes (adsorption, ion exchange) or chelation by the capsule polymers and subsequently the metal deposits themselves; (2) metal colloid aggregation; or (3) active biological uptake. First, capsules do present a tremendous surface area to their surrounding environment. Conservative estimates for the surface areas of single capsules were made using standard high resolution digital imaging techniques on TEM images. A typical value for a "Fibrous" capsule morph (3×10^3 $\mu m^2 cap^{-1}$) was over 3 orders of magnitude greater than the surface area of a 0.5 μm diameter sphere (0.8 $\mu m^2 cell^{-1}$), the size of a typical uncapsuled plume bacteria. The resulting total surface area represented by capsules in the plume water were estimated to be on the order of 10^7 to 10^8 μm^2 ml^{-1} depending on the concentration of capsules (Fig. 5).

In comparison, Sung and Morgan (1981) estimated (BET N_2 method) that a 1 mM L^{-1} solution of FeOOH would have a surface area of about 180 $m^2 g^{-1}$, or 10^6 to 10^7 $\mu m^2 ml^{-1}$ for 10 to 100 nM L^{-1} solutions. This is either less than or roughly equal to the surface area for the capsule population as estimated above. However, our own estimates yielded considerably higher surface areas for Fe oxide particles suspended in the plume. Our calculations were based on our direct observations (electron microscopy) of plume particles retained on 0.2 μm Nuclepore filters. A heavily loaded 0.2 μm filter retains a significant fraction of particles with diameters of 0.1 μm or smaller. The calculations yielded values on the order of 10^{11} to 10^{10} μm^2 ml^{-1} for surface areas contributed by FeOOH particles at PFe concentrations of 100 and 7 nM l^{-1}, respectively, assuming a particle diameter of 0.1 μm and a specific density of 2.4 g ml^{-1} for amorphous iron oxides. These PFe concentrations are typical of those found at plume depths of on- and most off-axis stations, respectively.

Therefore, the plume FeOOH particle population may have equal or much greater total surface area than the capsule population. Hence, surface area alone cannot account for the selective association of Mn with bacterial capsules. The high concentration of Mn with the bacterial capsules may suggest that the bacterial capsules also have a high physicochemical affinity for Mn relative to other particles in the samples studied. The primary capsule matrix consists of polyanionic polysaccharide and polypeptide polymers (Ghiorse and Hirsch, 1979). The strong binding of ruthenium red, a polysaccharide-specific metal stain (Luft, 1966), to the capsule polymers after metal deposit removal confirms the presence of polysaccharides.

Secondly, it is conceivable that capsules provide an effective aggregation mechanism for colloid size metal particles, thereby facilitating the transition between initial sorption by colloids to filterable particle size. If so, the Mn-colloids must be distinct from the Fe-colloids, otherwise no mass concentration difference for Mn would have been observed between the capsule Mn deposits and the Fe-colloids analyzed. The

capsule Mn:Fe ratio in previous studies increased significantly with increasing distance from plume origins (Cowen *et al.,* 1986) and with increasing apparent plume "age" (J.P.C., unpublished data) in two episodic "Megaplume" events (Baker *et al.,* 1989). Total particulate Mn:Fe ratios also increase with distance or apparent plume age (G. J. Massoth, unpublished data). However, this scenario does not explain differences in Mn:Fe ratios found between capsule morphs nor the absence of Mn-rich colloid like particles in the filtered particle samples similar to the amorphous FeOOH microparticles commonly observed.

Thirdly, evidence from several studies suggests that the bacteria do actively mediate the uptake of Mn. Certainly they do in the sense that excellent surface substrates for scavenging are produced, i.e. the capsules themselves. Other studies indicate a more active metabolic rate. Laboratory studies have shown that the addition of metabolic poisons inhibits Mn deposition but not Fe deposition (Ghiorse and Hirsh, 1979). Arcuri and Ehrlich (1979) demonstrated the involvement of cytochrome c (its reduction) in Mn (II) oxidation by two marine bacteria. Both studies suggested that Mn oxidation and its subsequent deposition are metabolically related to cell viability. In field studies, Mn binding onto particles, but not Fe binding, were also inhibited by metabolic poisons (Emerson *et al.,* 1982; Cowen *et al.,* 1986, 1990). At the least, it appears that the microbial mediation in Mn scavenging is a continuous process.

4. Conclusion

In conclusion, the results of our field studies support the contention that trace metal scavenging by particles is strongly influenced by the nature of the particles and not solely by particle mass. In the present case, it also appears that reliance on bulk analyses can be misleading when interpreted in terms of scavenging mechanisms (i.e., biogenic versus abiogenic; organic coated surfaces, $CaCO_2$, oxides, Al-silicates etc). If bacterial biomass can be taken as an indicator of trends in total particulate organic carbon (POC) in deep-sea plumes, then capsule-Mn would show no (or an inverse) correlation with total POC. Therefore, since our data suggest that most of the particulate Mn in the plumes is capsule-bound, particulate Mn should also show no positive correlation with POC. This correlation, however, could lead to the incorrect conclusion that the particulate Mn is not associated with biogenic phases. On the contrary, the data strongly support a formation (scavenging) mechanism dependent upon the local microbial population.

Acknowledgments. The authors gratefully acknowledge the microanalysis efforts of Thomas Ingledue III and the field and laboratory assistance of Ingledue, Naomi Okazaki and Donald McGee (SOEST Analytical EM Laboratory). We also greatly benefitted from the support of and discussions with Gary Massoth, Bill Lavelle, Richard Feely and Ed Baker of PMEL/ NOAA. This work was supported by NSF (OCE8711786 to JPC) and the Pacific Marine

Environmental Laboratory under the NOAA VENTS Program. SOEST Contribution no. 2626.

REFERENCES

Arcuri, E. J. and H. L. Ehrlich. 1979. Cylochrome involvement in Mn(II) oxidation by two marine bacteria. Appl. Environ. Microbiol. *37,* 916–923.

Bacon, M. P. and R. F. Anderson. 1982. Distribution of thorium isotopes between dissolved and particulate forms in the deep sea. J. Geophys. Res., *87,* 2045–2056.

Baker, E. T., J. W. Lavelle and G. J. Massoth. 1985. Hydrothermal particle plumes over the southern Juan de Fuca Ridge. Nature, *316,* 342–344.

Baker, E. T. and G. J. Massoth. 1986. Hydrothermal plume measurements: a regional perspective. Science, *234,* 980–982.

Baker, E. T., G. J. Massoth and R. A. Feely. 1987. Cataclysmic hydrothermal venting on the Juan de Fuca Ridge. Nature, *329,* 149–151.

Baker, E. T., J. W. Lavelle, R. A. Feely, G. J. Massoth, S. L. Walker and J. E. Lupton. 1989. Episodic venting of hydrothermal fluids from the Juan de Fuca Ridge. J. Geophys. Res., *94,* 9237–9250.

Balistrieri, L., P. G. Brewer and J. W. Murray. 1981. Scavenging residence times of trace, metals and surface chemistry of sinking particles in the deep ocean. Deep-Sea Res., *28,* 101–121.

Balistrieri, L. and J. W. Murray. 1984. Marine scavenging: Trace metal adsorption by interfacial sediment from MANOP Site H[1]. Geochim. et Cosmochim. Acta, *48,* 921–929.

—— 1986. The surface chemistry of sediments from the Panama Basin: the influence of Mn oxides on metal adsorption. Geochim. Cosmochim. Acta, *50,* 2235–2243.

Bishop, J. K. B. and M. Q. Fleischer. 1987. Particulate manganese dynamics in Gulf Stream warm-core rings and surrounding waters of the N.W. Atlantic. Geochim. Cosmochim. Acta, *51,* 2807–2825.

Bolger, G. W., P. R. Betzer and V. V. Gordon. 1978. Hydrothermally-derived manganese suspended over the Galapagos spreading center. Deep-Sea Res., *25,* 721–33.

Cannon, G. A., D. J. Pashinski and M. Lemon. 1991. Mid-depth flow near hydrothermal venting sites on the southern Juan de Fuca Ridge. J. Geophys. Res., (in press).

Coale, K. H. and K. W. Bruland. 1985. ^{234}Th:^{238}U disequilibria within the California Current. Limnol. Oceanogr., *30,* 22–33.

Costerton, J. W., R. T. Irwin and K. J. Cheng. 1981. The bacterial glycocalyx in nature and disease. Annu. Rev. Microbiol., *35,* 299.

Cowen, J. P. 1989. Positive pressure effect on manganese binding by bacteria in deep-sea hydrothermal plumes. Appl. and Environ. Microbiol., *55(3),* 764–766.

Cowen, J. P. and K. W. Bruland. 1985. Metal deposits associated with bacteria: Implications for Fe and Mn marine biogeochemistry. Deep-Sea Res., *32,* 253–272.

Cowen, J. P., G. J. Massoth and E. T. Baker. 1986. Bacterial scavenging of Mn and Fe in a mid- to far-field hydrothermal particle plume. Nature, *322,* 169–171.

Cowen, J. P., G. J. Massoth and R. A. Feely. 1990. Scavenging rates of dissolved manganese in a hydrothermal vent plume. Deep-Sea Res., *37,* 1619–1637.

Cowen, J. P. and M. W. Silver. 1984. The association of iron and manganese with bacteria on marine macroparticulate material. Science, *224,* 1340–1342.

Davis, J. A. and J. O. Leckie. 1979. Surface ionization and complexation at the oxide/water interface. J. Colloid. Inter. Sci., *67,* 90–107.

Di Toro, D. M., J. D. Mahony, P. R. Kirchgraber, A. L. O. Bryne, L. R. Pasquale and D. C. Piccirilli. 1986. Effects of nonreversibility, particle concentration and ionic strength on heavy metal adsorption. Environ. Sci. Technol., *20,* 50–61.

Embley, R. W., S. Hammond, K. Murphy, C. Fox, B. Applegate, G. Massoth, R. Feely, E. Baker, J. Gendron, G. Lebon, D. Butterfield, B. Coughkin, J. Lupton, I. Jonasson, M. Perfit, J. Cowen, V. Tunnicliffe and A. Tuivett. 1988. Submersible observation of "Megaplume" area: Southern Juan de Fuca Ridge. EOS, *69,* 1497.

Emerson, S., S. Kalhorn, L. Jacobs, B. M. Tebo, K. H. Nealson and R. A. Rosson. 1982. Environmental oxidation rate of Manganese (II): Bacterial catalysis. Geochem. Cosmochim. Acta, *46,* 1073–1079.

Feely, R. A., G. J. Massoth, E. T. Baker, J. P. Cowen, M. F. Lamb and K. A. Krogslund. 1990. The effect of hydrothermal processes on midwater phosphorus distributions in the Northeast Pacific. Earth Planet. Sci. Lett., *96,* 305–318.

Ghiorse, W. C. and P. Hirsch. 1979. An ultrastructural study of Fe and Mn deposition associated with extracellular polymers of pedomicrobium-like budding bacteria. Arch. Microbiol., *123,* 213–226.

Hall, T. A. 1971. The microprobe assay of chemical elements, *in* Physical Techniques in Biological Research, G. Oster, ed., 2nd ed, Vol-IA, PP- 157–275. Academic Press, NY.

—— 1979a. Biological X-ray microanalysis. J. Microsc., *117,* 145–63.

—— 1979b. Problems of the continuum-normalization method for the quantitative analysis of sections of soft tissue, *in* Microbeam Analysis in Biology, C. Lechene and R. Warner, eds., Academic Press, NY, 185–202.

Hall, T. A. and B. L. Gupta. 1979. EDS quantitation and application to biology, *in* Introduction to Analytical Electron Microscopy, J. J. Hren, J. I. Goldstein, and D. C. Joy, eds., Plenum Press, New York, London, 169–97.

Hastings, D. and S. Emerson. 1986. MnII oxidation by spores of a marine *Bacillus:* Kinetic and thermodynamic considerations. Geochem. Cosmochim. Acta, *50,* 819.

Higgo, J. J. W. and L. V. C. Rees. 1986. Adsorption of actinides by marine sediments: Effect of the sediment/seawater ratio on the measured distribution coefficient. Environ. Sci. Technol., *20,* 483–490.

Honeyman, B. O., A. W. Adamson and J. W. Murray. 1988a. Panel 2: The nature of reactions on marine particle surfaces. Appl. Geochem., *3,* 19–26.

Honeyman, B. D., L. S. Balistrieri and J. W. Murray. 1988b. Oceanic trace metal scavenging: the importance of particle concentration. Deep-Sea Res., *35,* 227–246.

Honeyman, B. D. and P. H. Santschi. 1988. Metals in aquatic systems. Environ. Sci. & Technol., *22,* 862–871.

—— 1989. A brownian-pumping model for oceanic trace metal scavenging Evidence from Th isotopes. J. Mar. Res., *47,* 951–992.

Jannasch, H. W., B. D. Honeyman, L. S. Balistrieri and J. W. Murray. 1988. Kinetics of trace element uptake by marine particles. Geochim. et Cosmochim. Acta, *52,* 567–577.

Karl, D. M., C. O. Wirsen and H. W. Jannasch. 1980. Deep-sea primary production at the galapagos hydrothermal vents. Science, *207,* 1345–1347.

Klinkhammer, G., H. Elderfield, M. Greaves, P. Rona and T. Nelsen. 1980. Manganese geochemistry near hightemperature vents in the Mid-Atlantic Ridge rift valley. Earth Planet. Sci. Lett., *80,* 230–240.

Klinkhammer, G. and A. Hudson. 1986. Dispersal patterns for hydrothermal plumes in the South Pacific using manganese as a tracer. Earth Planet. Sci. Lett., *79,* 241–249.

Klinkhammer, G., P. Rona, M. Greaves and H. Elderfield. 1985. Hydrothermal manganese plumes in the Mid-Atlantic Ridge rift valley. Nature, *314,* 722–731.

Koppel, E. J. and W. R. Normark. 1987. Morphometric variability within the axial zone of the Southern Juan de Fuca Ridge: interpretation from sea MARC II, Sea MARC I and deep sea photography. J. Geophys. Res., *92,* 11, 291–11,302.

Koppel, E. J. and W. B. F. Ryan. 1986. Volcanic episodiaty and a nonsteady state rift valley along northeast Pacific spreading centers: evidence from Sea MARC I. J. Geophys. Res., *91,* 13, 925–13,940.

Landing, W. M. and K. W. Bruland. 1987. The contrasting biogeochemistry of iron and manganese in the Pacific Ocean. Geochim. et Cosmochim. Acta, *51,* 29–43.

Li, Y.-H., L. Burkhardt, M. Buchholtz, P. O'Hara and P. Santchi. 1984. Partition of radiotracers between suspended particles seawater. Geochim. Cosmochim. Acta, *48,* 2011–2019.

Loeb, G. I. and R. A. Neihoff. 1977. Adsorption of an organic film at a platinum seawater interface. J. Mar. Res., *35,* 283–291.

Luft, J. H. 1966. Ruthenium red staining of the striated muscle cell membrane and the myotendinal junction, *in* Sixth Intern. Congress for Electron Microscopy, Kyoto.

Lupton, J. E., J. R. Delaney, H. P. Johnson and M. K. Tivey. 1985. Entrainment and vertical transport of deep-ocean water by buoyant hydrothermal plumes. Nature, *316,* 621–623.

Mandernack, K. W. and B. M. Tebo. 1988. Manganese scavenging and oxidation at hydrothermal vents and in vent plumes. EOS, *69,* 1094.

Massoth, G. J., E. T. Baker, R. A. Feely, J. E. Lupton, D. A. Butterfield and R. E. Meduff. 1988. Hydrothermal Fluids and Plumes of Cleft Segment, Juan de Fuca Ridge. EOS, *69,* 1497.

Morel, F. M. M. and P. M. Gschwend. 1987. The role of colloids in the partitioning of solutes in natural waters, *in* Aquatic Surface Chemistry: Chemical Processes at the Particle-Water Interface, Chapter 15, W. Stumm, ed., John Wiley, NY.

Nealson, K. H. 1983. The microbial manganese cycle, *in* Microbial Geochemistry: Studies in Microbiology, Vol. 3, W. E. Krumbein, ed., Blackwell Press. Oxford, 191–221.

Neihof, R. A. and G. Loeb. 1974. Dissolved organic matter in seawater and the electric charge of immersed surfaces. J. Mar. Res., *32,* 5–12.

Normark, W. R., J. L. Morton, R. A. Koski, D. A. Clague and J. R. Delaney. 1983. Active hydrothermal vents and sulfide deposits on the southern Juan de Fuca Ridge. Geology, *11,* 158–163.

Normark, W. R., J. L. Morton and S. L. Ross. 1987. Submersible observations along the southern Juan de Fuca Ridge: 1984 *Alvin* program. J. Geophys. Res., *92,* 11,283–11,290.

Nyffeler, U. P., Y. H. Li and P. H. Santschi. 1984. A kinetic approach to describe trace element distribution between particles and solution in natural aquatic systems. Geochim. Cosmochim. Acta, *48,* 1513–1522.

Porter, K. G. and Y. S. Feig. 1980. The use of DAPI for identifying and counting aquatic microflora. Limnol. Oceanogr., *25,* 943–948.

Ringo, D. L., E. H. Cota-Robles and B. J. Humphrey. 1979. Low viscosity embedding resins for TEM. 37th Annual Proceedings Electron Microscopy Society of America. San Antonio, Texas. G. W. Barley, ed., 348–349.

Silver, M. W. and K. W. Bruland. 1981. Differential feeding and fecal pellet composition of salps and pteropods, and the possible origin of the deep-water flora and olive-green "cells." Mar. Biol., *62,* 263–273.

Stumm, W. and J. J. Morgan. 1981. Aquatic Chemistry. 2nd ed. John Wiley & Sons, NY, 780 pp.

Sunda, W. G. and S. A. Huntsman. 1988. Effect of sunlight on redox cycles of manganese in the southwestern Sargasso Sea. Deep-Sea Res., *35,* 1297–1317.

Sung, W. and J. J. Morgan. 1981. Oxidative removal of Mn(II) from solution catalyzed by the *y*-FeOOH (lepidocrocite) surface. Geochim. et Cosmochim. Acta, *45,* 2377–2383.

Tebo, B. M. and S. Emerson. 1985. Effect of oxygen tension, Mn(II) concentration, and temperature on microbially catalyzed Mn(II) oxidation rate in a marine fjord. Appl. Environ. Microbiol., *50,* 1268–1273.

Tebo, B. M., K. H. Nealson, S. Emerson and L. Jacobs. 1984. Microbial mediation of Mn(II) and Co(II) precipitation at the O2/H2S interfaces in two anoxic fjords. Limnol. Oceanogr., *29,* 1247–1258.

Tuttle, J. H., C. O. Wirsen and H. W. Jannasch. 1983. Microbial activities in the emitted hydrothermal waters of the Galapagos Rift vents. Mar. Biol., *73,* 293–299.

USGS Juan de Fuca Group. 1986. Submarine fissure eruptions and hydrothermal vents on the southern Juan de Fuca Ridge: preliminary observations from the submersible *Alvin. Geology, 14,* 823–827.

Winn, C. K., D. M. Karl and G. J. Massoth. 1986. Microorganisms in deep-sea hydrothermal plumes. Nature, *320,* 744–746.

Received: *19 June, 1990;* revised: *14 May, 1991.*